Polym. Bull. (2012) 68:815–827
DOI 10.1007/s00289-011-0595-8

ORIGINAL PAPER

Dynamic mechanical behavior of mPE/mEP blends: experimental and prediction

Xuhuang Chen · Peng Yu · Biwei Huang · Peng Long

Received: 29 November 2010 / Revised: 26 May 2011 / Accepted: 31 July 2011 /
Published online: 11 August 2011
© Springer-Verlag 2011

Abstract Metallocene-catalyzed polyethylene (mPE)/metallocene-catalyzed ethylene–propylene copolymer (mEP) blends were prepared with a mixing apparatus. The morphology of the blends was observed by scanning electron microscopy and the dynamic mechanical behavior of the blends was systematically investigated. Mean-field theories developed by Kerner were applied to these binary blends of different compositions. The Kerner's model calculations were compared with the experimental dynamic mechanical properties of the blends and their morphological characterizations. The results showed that Kerner's model can reasonably predict the viscoelasticity of mPE/mEP blends with different compositions. In addition, the morphological structure of the blends can be estimated via comparing the predicted dynamic mechanical behavior with the experimental data.

Keywords Metallocene-catalyzed polyethylene (mPE) · Metallocene-catalyzed ethylene–propylene copolymer (mEP) · Dynamic mechanical properties · Kerner's model · Viscoelastic properties

Introduction

Blending of polymers is a common, economical practice in the polymer industry to meet the specific demands for new materials. Most polymer blends are immiscible; however, even phase-separated blends prove to be mechanically compatible provided that adequate adhesion exists between the phases. Compatible polymer blends provide opportunities of attaining advantageous mechanical properties which are superior to those available with the individual component polymers.

X. Chen (✉) · P. Yu · B. Huang · P. Long
School of Chemical and Environmental Engineering, Hubei University of Technology, Wuhan 430068, People's Republic of China
e-mail: cxh213@126.com

The metallocene catalyst yields polyolefins with narrow molecular-weight distribution, bimodal or trimodal, whereas the conventional Ziegler–Natta catalyst produces a relatively broad distribution of molecular weights. Metallocene polymers often have poor processability due to their high viscosity, whereas they exhibit better physical and mechanical properties than their conventional counterparts with the same average molecular weight. Polyethylenes are plastic materials with the most diversified uses in the industry; and, the newest member of this family is a polyethylene synthesized by constrained geometry metallocene catalyst technology. This new class of polyethylene exhibits a molecular structure with narrow molecular-weight distribution and uniformity of comonomer distribution, and often offers unique mechanical and rheological properties. Numerous investigations have been conducted to characterize chain structures and relaxation properties [1–14]. Metallocene-catalyzed ethylene–propylene copolymer is an elastomer that can be widely used to toughen olefinic polymers such as polypropylene and polyethylene [15–17]. Because of high incorporation of α-olefin with metallocene catalysts, metallocene copolymers have low crystallinity. A high energy dissipation (tan δ) at low temperatures has been observed by dynamic mechanical analysis (DMA) [1–4]. The influence of α-olefin incorporation on polymer properties is more apparent with polymers in crystalline state than in melt. In molten state, metallocene polymers with narrow molecular-weight distribution exhibit poor shear-thinning behavior.

Viscoelastic behavior characterized by DMA has dominant effects on mechanical properties of polymers and their blends. On the other hand, application of theoretical models, which aim at understanding and predicting the mechanical behavior and morphology of the blends from the individual component characteristics, has gained attention [18]. Computation modeling is widely used to calculate the viscoelastic properties of the blends, based on the measured properties of the individual components and theoretical models such as mechanical coupling, mean-field, bounding, and semi-empirical models [19, 20]. Especially, the mean-field theories developed by Kerner are usually applied to predicting the viscoelastic properties of polymer blends [21, 22]. In this article, the dynamic mechanical behavior of (metallocene-catalyzed polyethylene)/(metallocene-catalyzed ethylene–propylene copolymer) blends will be systematically studied experimentally, and their viscoelastic properties will be predicted by means of Kerner's model.

Experimental

Materials

Metallocene-catalyzed polyethylene (mPE, Exceed-2018CA) is a commercial polymer from ExxonMobil Corporation. (USA), with $\rho = 0.918$ g/cm^3 and MI (melt index) = 2.0 g/10 min (2.16 kg, 230 °C). The elastomer, a copolymer of ethylene and propylene synthesized with metallocene catalyst (mEP, Vistamaxx VMX-6202) is a commercial material from ExxonMobil Corporation. (USA), with $\rho = 0.861$ g/cm^3 and MI = 7.4 g/10 min (2.16 kg, 190 °C).

Specimen preparation

The compositions of the blends were 80/20, 70/30, 60/40, 50/50, 40/60, and 20/80 (mPE/mEP v/v). Binary preblends of mPE and mEP were made by melt-mixing the components in a mixing apparatus (SU-70 internal mixer, working cubage is 70 mL, China) at a temperature of 180 °C with fixed time (10 min) and rotational speed (36 rpm). The preblend samples were rapidly immersed in liquid nitrogen, removed after 2 h, and fractured. The cryo-fractured surfaces were etched with cyclohexane prior to examination by scanning electron microscopy (SEM). All of the preblends were then melt-compounded in a single-screw extruder (30/25, Wuhan Plastics Machinery Factory, China) at a screw speed of 50 rpm. The barrel temperature profile was set to 160, 170, and 180 °C, respectively. The extrudates were pelletized by comminutor, then dried, and finally injection-molded to standard unnotched Izod impact specimens ($60 \times 60 \times 4$ mm^3) by an injection molding machine (TY-200, Hangzhou Dayu Plastics Machinery Co. Ltd., China), whose barrel temperature profile was set to 170, 175, and 180 °C, respectively.

Dynamic mechanical analysis (DMA)

DMA was conducted with a dynamic mechanical analyzer (Q800, TA Instruments) at a constant frequency of 1 Hz and a strain amplitude of 15 μm (0.01%) in the dual cantilever clamp mode (blending mode). The temperature range was from −80 to 120 °C at a heating rate of 3 °C/min. The dimension of the test specimens was $60 \times 60 \times 4$ mm^3.

Scanning electron microscopy (SEM)

The morphologies of the blends were observed under a scanning electron microscope (6390LV, JEOL JSM, Japan) at an acceleration voltage of 20 kV and a magnification of 3,000. The cryo-fractured surface of each specimen was etched by cyclohexane at room temperature for 30 min in order to remove the mEP phase. Then, the fracture surfaces of the specimens were coated with a thin layer of gold for microscopic observation, to insure that the etched surface structure of the blends was intact.

Results and discussion

Etching of microscopically cryo-fractured surfaces of the blends with cyclohexane removed the elastomer component, leaving dark holes. Figure 1 shows SEM images of mPE/mEP blends with different mEP contents. When the mEP content is lower than 40% (volume fraction), the elastomer (mEP) component is the dispersed phase corresponding to the uniformly distributed cavities. With increasing the mEP content, the average diameter of mEP domains increases from 0.54 μm for the mPE/mEP (80/20) blend to 1.04 μm for the mPE/mEP (70/30) blend, and their distributions are uniform, as shown in Fig. 1a and b. This indicates that there may

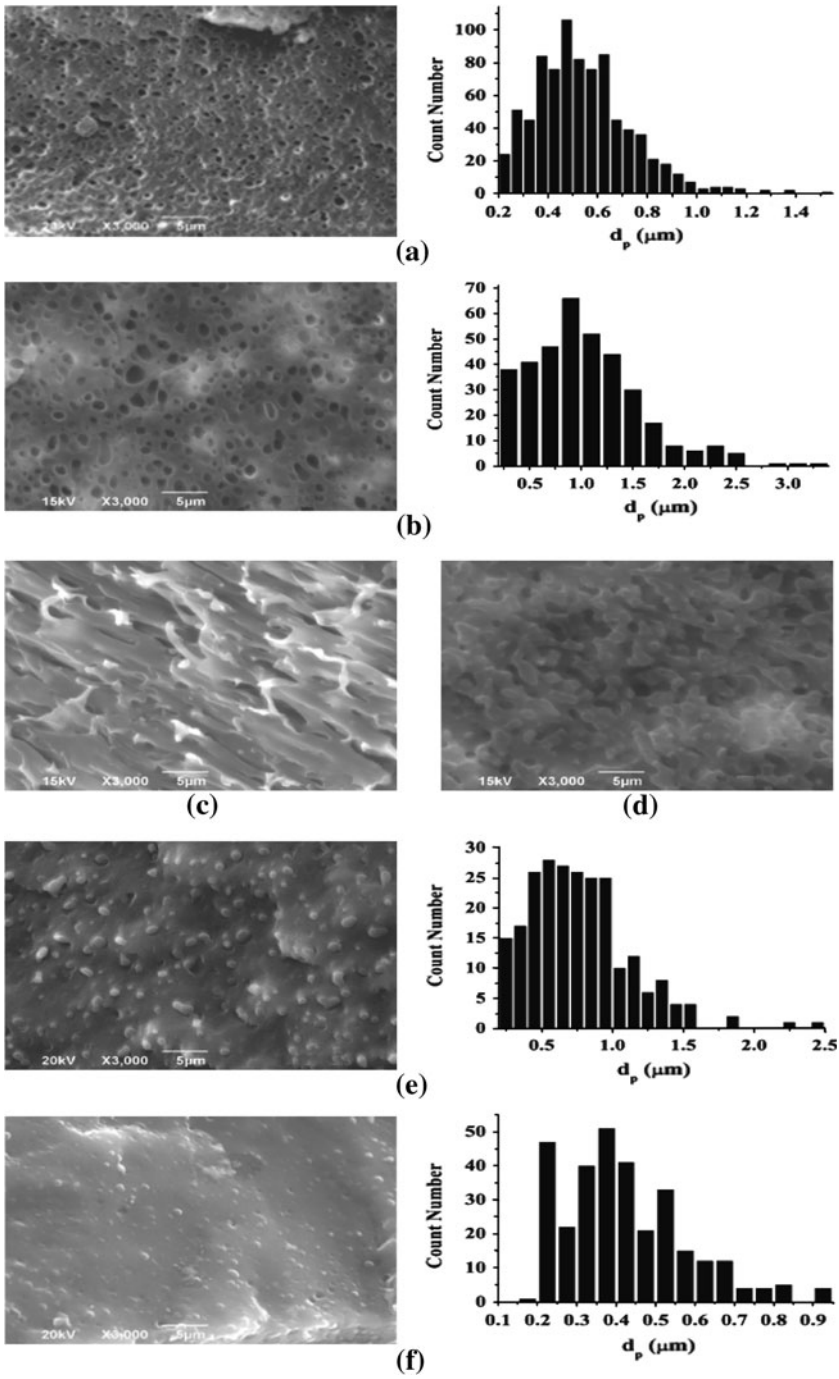

Fig. 1 SEM images of mPE/mEP blends with different compositions. **a** mPE/mEP (80/20), **b** mPE/mEP (70/30), **c** mPE/mEP (60/40), **d** mPE/mEP (50/50), **e** mPE/mEP (40/60), **f** mPE/mEP (20/80)

be a strong interaction between mPE matrix and dispersed mEP phase, which leads to the uniform dispersion of mEP in mPE matrix. When the mEP content is between 40 and 50%, the blends exhibit co-continuous phase structures. As expected, when the mEP content is more than 60%, phase inversion occurs in the mPE/mEP (40/60) blend, where mPE is the dispersed phase corresponding to the spherical (or ellipsoidal) protuberances distributed uniformly throughout the sample. With increasing the mPE content, the average diameter of mPE domains increases from 0.42 μm for the mPE/mEP (20/80) blend to 0.77 μm for the mPE/mEP (40/60) blend, and the number of particles reduces from 312 in Fig. 1f to 237 in Fig. 1e. This indicates that the collision probability of the particles increases due to increasing the dispersed-phase content, which leads to a decrease in the number of particles and an increase in the domain size.

Morphologies of mPE/mEP blends

Dynamic mechanical properties

The dynamic mechanical methods based on oscillatory disturbances, such as sinusoidal strains, to create resonance with molecular motions are widely used to characterize the viscoelastic properties, thermal transitions and relaxation behavior of polymers. The resulting viscoelastic parameters are expressed as follows:

$$E^* = E' + iE'' \tag{1}$$

$$\tan\delta = E''/E' \tag{2}$$

where E^*, E', and E'' are complex, storage, and loss moduli, respectively, δ is the phase angle, and tan δ is loss tangent (or loss factor), which reflects the magnitude of mechanical loss and is associated with the mobility of polymer chain segments.

Figure 2 shows the variations of storage modulus (E') with temperature for mPE/mEP blends including pure component polymers. Obviously, the E' value of pure mEP is higher than that of pure mPE below the glass transition temperatures (T_g's) of both polymers, due to the higher molecular weight of mEP than mPE. For example, the E' values of mPE and mEP at −60 °C are 6,485 and 11,157 MPa, respectively, where mPE and mEP are in glassy state. However, at higher temperatures, such as 60 °C, their E' values are close to each other because they are in highly elastic state. From Fig. 2, it can be seen that the E' value of mPE/mEP blends increases with the addition of mEP content below the T_g's. Moreover, the E' value of pure mEP shows a sharp drop in its glass transition region, while that of pure mPE exhibits a gradual decrease across its glass transition region due to the existence of crystalline structure in mPE, which restricts the mobility of amorphous chain segments. With increasing the mPE content, the E' value of the blends decreases more gently with the increase of temperature.

Loss modulus (E''), referred to as "internal friction," is an important characteristic of polymer materials, which is associated with their viscoelasticity. Figure 3 shows the variations of E'' with temperature for mPE/mEP blends including pure component polymers. Obviously, the loss peaks of pure mPE and mEP occur at

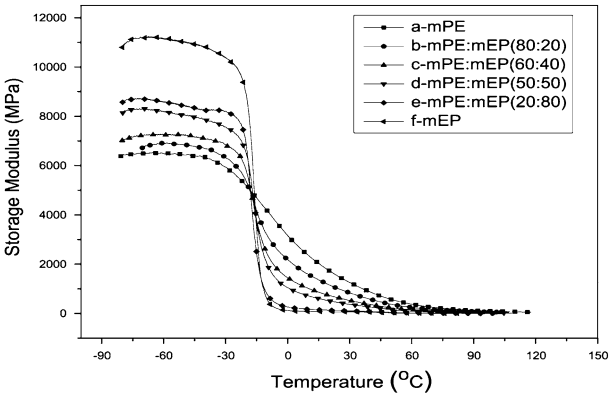

Fig. 2 Variations of storage modulus with temperature for different compositions of mPE/mEP blends

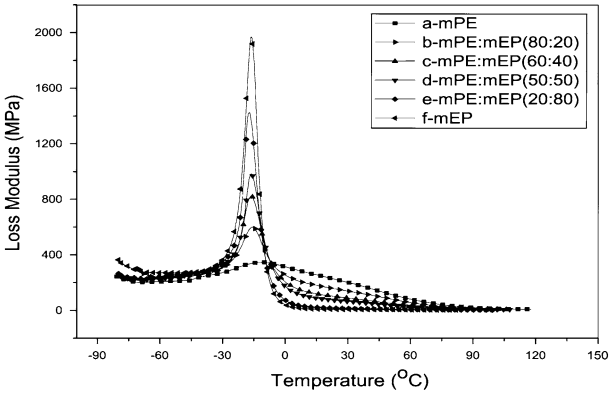

Fig. 3 Variations of loss modulus with temperature for different compositions of mPE/mEP blends

about −9.94 and −16.29 °C, respectively, which correspond to their T_g's. Noticeably, mPE/mEP blends exhibit only one glass transition peak. Furthermore, with increasing the mEP content, the loss peak becomes sharper, and the peak point (T_g) shifts toward lower temperatures. These are due to the diminution of crystalline structure of mPE upon the addition of mEP: the flexible chain segments of mEP lead to an increase in the entanglement points, which causes the E'' to be higher because of greater internal friction during the motion of the entangled chains.

Prediction of the viscoelastic behavior of mPE/mEP blends

Early in 1956, Kerner [21] developed the mean-field theories to predict the viscoelastic properties of polymer blends. He put forward Kerner's dispersed-phase model which assumes one of the components in the blend to be the matrix and the others to be dispersed inclusions, and co-continuous-phase model which assumes

neither of the components to be the matrix but the blend approximates a co-continuous structure.

The assumptions underlying the dispersed-phase model are that spherical inclusions of varying sizes are randomly distributed in the volume of the matrix; and that the phase surfaces are in direct contact (bonded physically or chemically), that is, there is no slip at the phase interfaces, but interactions between particles are ignored. The model gives the overall average response of the material to loads (or deformation) rather than localized variation in material characteristics. The model for predicting the shear modulus of a multicomponent system is as follows:

$$\frac{G^*}{G_{\mathrm{m}}^*} = \frac{\sum_{i=1}^{n} \frac{G_i^* \phi_i}{[(7-5\upsilon_{\mathrm{m}})G_{\mathrm{m}}^* + (8-10\upsilon_{\mathrm{m}})G_i^*]} + \frac{\phi_{\mathrm{m}}}{15(1-\upsilon_{\mathrm{m}})}}{\sum_{i=1}^{n} \frac{G_{\mathrm{m}}^* \phi_i}{[(7-5\upsilon_{\mathrm{m}})G_{\mathrm{m}}^* + (8-10\upsilon_{\mathrm{m}})G_i^*]} + \frac{\phi_{\mathrm{m}}}{15(1-\upsilon_{\mathrm{m}})}} \tag{3}$$

where i is 1, 2, 3, …, n (number of dispersed-phase components), G^* is the complex shear modulus of the blend, G_{m}^* is the complex shear modulus of the matrix, G_i^* is the complex shear modulus of the dispersed-phase component, υ_{m} is the Poisson ratio of the matrix, ϕ_i is the volume fraction of the dispersed-phase component, and ϕ_{m} is the volume fraction of the matrix. The Kerner equation which for a binary blend of viscoelastic materials can be adapted for the complex Young's modulus through the correspondence principle and the relation $E^* = 2(1 + \upsilon^*)G^*$, where $\upsilon^* = \upsilon'\upsilon''$ is the viscoelastic Poisson ratio. Here, υ^* is assumed as υ' (a real quantity), that is, the elastic Poisson ratio. The transformed equation is represented as follows:

$$\frac{E^*}{E_{\mathrm{m}}^*} = \gamma \frac{(1-\phi_i)E_{\mathrm{m}}^* + \beta(\alpha+\phi_i)E_i^*}{(1+\alpha\phi_i)E_{\mathrm{m}}^* + \alpha\beta(1-\phi_i)E_i^*} \tag{4}$$

where $\alpha = 2(4 - 5\upsilon_{\mathrm{m}})/(7 - 5\upsilon_{\mathrm{m}})$; $\beta = (1 + \upsilon_{\mathrm{m}})/(1 + \upsilon_{\mathrm{i}})$ and $\gamma = (1 + \upsilon)/(1 + \upsilon_{\mathrm{m}})$; υ is the Poisson ratio of the blend, υ_{m} is the Poisson ratio of the matrix, and υ_i is the Poisson ratio of the dispersed inclusion.

In computing the viscoelastic properties of mPE/mEP blends, E', E'', and tan δ of the two pure components, mPE and mEP, are obtained experimentally from DMA. Poisson ratio (υ) of polymers generally varies from 0.32 to 0.5 (glassy plastic to rubbery zone), and its variation with temperature can be calculated by means of Mazich equation [22, 23]:

$$\upsilon(T) = \frac{0.17[\lg G'_{\mathrm{glass}} - \lg G'(T)]}{\lg G'_{\mathrm{glass}} - \lg G'_{\mathrm{rubber}}} + 0.32 \tag{5}$$

Kerner's co-continuous-phase model assumes that particles of each component are suspended in a third component. As the concentration of the third component approaches zero, particles of each component will pack together in the volume of the material. The model for predicting the shear modulus of a binary blend is as follows:

$$\frac{(G^* - G_1^*)\phi_1}{(7-5\upsilon)G^* + (8-10\upsilon)G_1^*} + \frac{(G^* - G_2^*)\phi_2}{(7-5\upsilon)G^* + (8-10\upsilon)G_2^*} = 0 \tag{6}$$

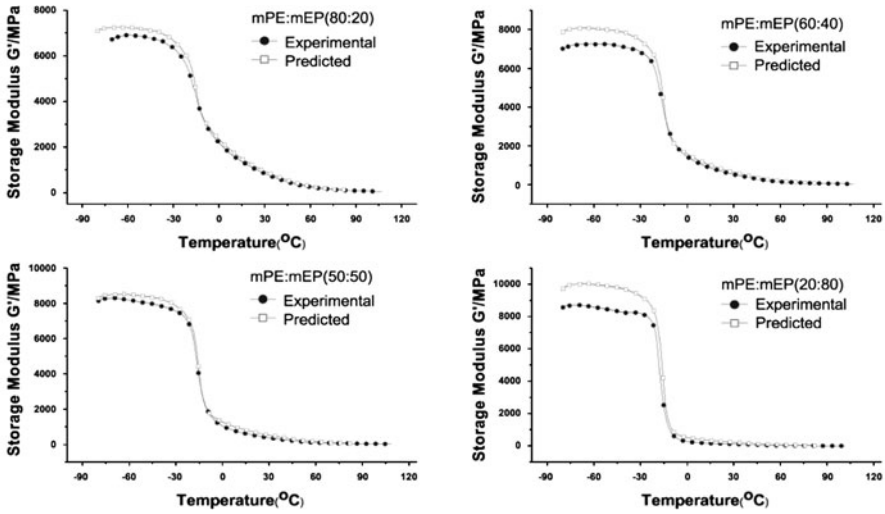

Fig. 4 Comparisons between the experimental and predicted data of storage modulus for mPE/mEP blends using Kerner's dispersed-phase model with mPE assumed as the matrix

where subscripts 1 and 2 represent components 1 and 2, respectively. Equation 6 can be expressed in terms of the dynamic Young's modulus (E'') through the equations $E^* = 2(1 + \upsilon^*)G^*$.

Figures 4 and 5 present the comparisons between the experimental and predicted data of storage modulus for mPE/mEP blends using Kerner's dispersed-phase model with mPE and mEP assumed as the matrix, respectively. As shown in Fig. 4, the predicted E' values for the mPE/mEP (80/20) blend are in good agreement with the experimental data in the entire temperature range studied. Differences between the predicted and experimental data are observed below the T_g, where the predicted values are slightly higher than the experimental data. It is interesting to note that the dispersed-phase model assuming mPE as the matrix gives excellent prediction of the experimental data above the T_g for all the blends with different compositions. For the mPE/mEP (50/50) blend, it is also observed that the predictions with the model assuming mPE as the matrix are matched reasonably well to the experimental data in the entire temperature range. In Fig. 5, there is a satisfactory match between the experimental data and the predictions with the model assuming mEP as the matrix above the T_g for the mPE/mEP (20/80) blend. A deviation exists below the T_g, where the predicted values are considerably higher than the experimental data. Theoretical predictions are markedly different from the experimental data for other blends.

Figures 6 and 7 show the comparisons between the experimental and predicted loss-tangent data for mPE/mEP blends using Kerner's dispersed-phase model with mPE and mEP assumed as the matrix, respectively. It is observed from Fig. 6 that predictions provide a close match to the experimental data for the mPE/mEP (80/20) blend. The match is excellent below the T_g, while there is a small difference in the intensity of the peaks. The experimental peaks occur at slightly higher tan δ values

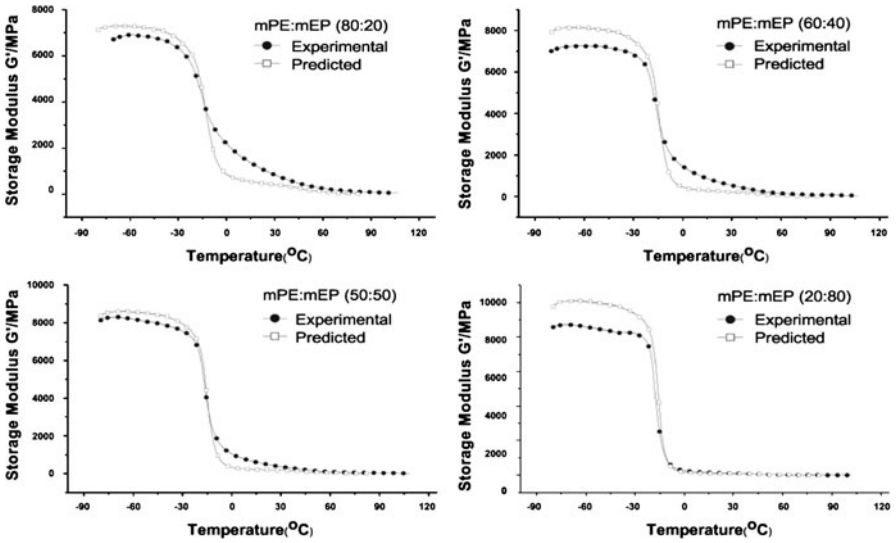

Fig. 5 Comparisons between the experimental and predicted data of storage modulus for mPE/mEP blends using Kerner's dispersed-phase model with mEP assumed as the matrix

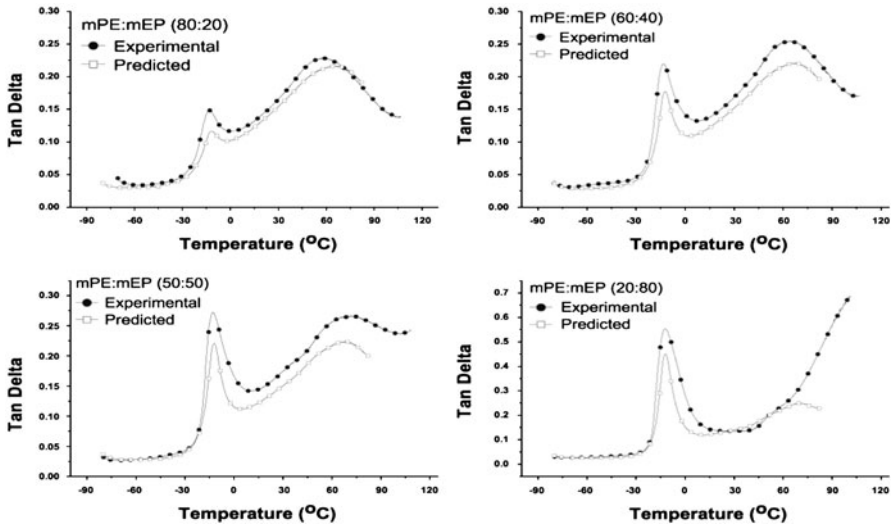

Fig. 6 Comparisons between the experimental and predicted loss-tangent data for mPE/mEP blends using Kerner's dispersed-phase model with mPE assumed as the matrix

than the predicted ones. Although the predicted values are marginally lower than the experimental data, they clearly indicate the trend of the experimental results, i.e., two transitions corresponding to the glass transition and the slip of crystal layers, respectively. Noticeably, below the T_g, a satisfactory match between the experimental data and the predictions is also observed in the case of other blends.

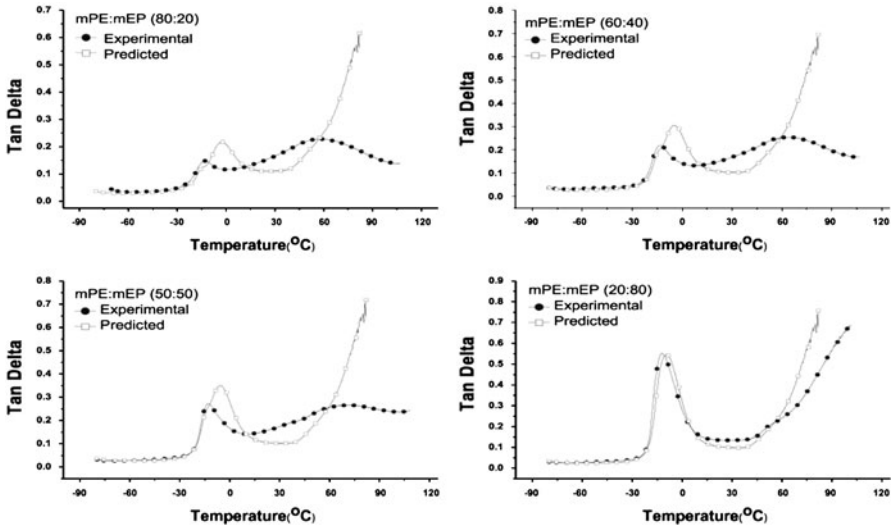

Fig. 7 Comparisons between the experimental and predicted loss-tangent data for mPE/mEP blends using Kerner's dispersed-phase model with mEP assumed as the matrix

A possible explanation is that the molecular motion is frozen in the low-temperature range, and both the components behave like elastic solids. In the temperature region between the two transition peaks, the mobility of chain segments just sets in. Thus, a good match is observed in the region. Deviation occurs at higher temperatures where long-range rubbery relaxations contribute. From Fig. 7, a satisfactory match is observed in that the predicted loss-tangent values are in excellent agreement with the experimental data for the mPE/mEP (20/80) blend. For other blends, there exist obvious differences between experimental and predicted data as temperature is increased beyond the T_g. The results are in conformity with SEM analysis of the blends, which indicates that Kerner's dispersed-phase model can reasonably predict the viscoelasticity of polymer blends.

Figures 8 and 9 show the comparisons between the experimental and predicted storage-modulus and loss-tangent data, respectively, for mPE/mEP blends using Kerner's co-continuous-phase model. It is observed from Fig. 8 that storage-modulus predictions based on the co-continuous model provide a close match to the experimental data for the mPE/mEP (50/50) and mPE/mEP (60/40) blends. The match is excellent above the T_g and in the T_g region. There are small differences below the T_g, where the predictions are slightly higher than the experimental data. For the mPE/mEP (80/20) blend, it is also observed that the co-continuous-phase model's predictions are in good match to the experimental data. However, the closeness of the co-continuous calculations to the experimental data is difficult to correspond with the SEM finding that the mPE/mEP (80/20) blend has a dispersed-phase morphology. A possible explanation is the volume fraction of the "packed grains" of the major component, mPE. The number of grains of mPE is sufficiently large enough to form a matrix for the grains of mEP. The lack of fit for the

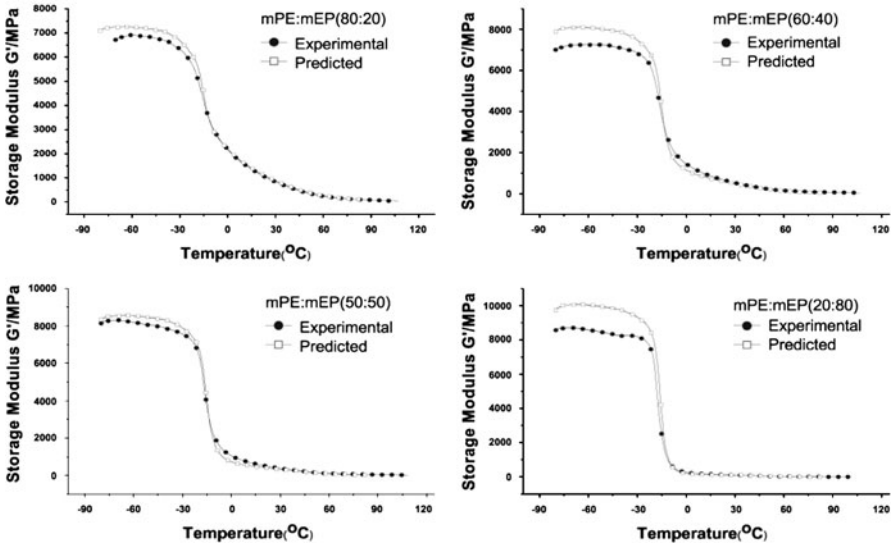

Fig. 8 Comparisons between the experimental and predicted storage-modulus data for mPE/mEP blends using Kerner's co-continuous-phase model

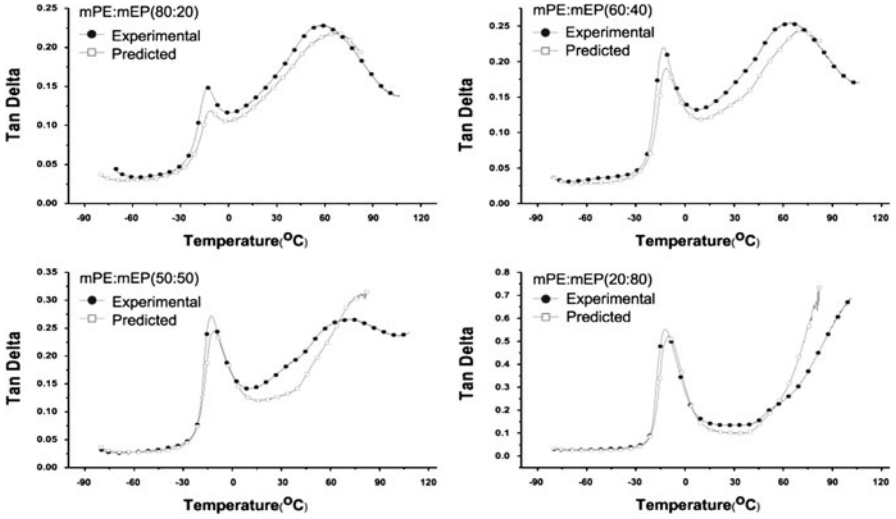

Fig. 9 Comparisons between the experimental and predicted loss-tangent data for mPE/mEP blends using Kerner's co-continuous-phase model

mPE/mEP (20/80) blend is in accordance with expectations. As shown in Fig. 9, the predicted loss-tangent values by Kerner's co-continuous-phase model are in good agreement with the experimental data below the T_g for the mPE/mEP (50/50) and mPE/mEP (60/40) blends. Noticeably, the predicted peaks are marginally lower than the experimental ones. It is interesting to note that the predicted values for the

mPE/mEP (20/80) blend give excellent agreement with the experimental data in the T_g region as well. A marked deviation exists, however, between the experimental data and the predicted values for the mPE/mEP (80/20) blend in the entire temperature range. The results are consistent with SEM analysis of the blends, which indicates the applicability of co-continuous-phase model to predicting the viscoelasticity of polymer blends.

Conclusions

The morphological structure of mPE/mEP blends with different compositions has been observed by SEM. The results show that mPE/mEP blends are heterogeneous. The Kerner's dispersed-phase model and co-continuous-phase model have been used to predict the viscoelastic properties of the mPE/mEP blends over a temperature range including the T_g regions of the individual components. The comparison of the experimental data and the predicted values indicates that Kerner's model can reasonably predict the viscoelasticity of mPE/mEP blends with different compositions. Additionally, the morphological structure of the blends estimated via comparing the predicted dynamic mechanical behavior with the experimental data is consistent with SEM analysis of the blends.

Acknowledgment The authors gratefully thank the Talent Foundation of Hubei University of Technology (contract grant number 2007D00001).

References

1. Woo L, Westphal S, Ling MTK (1994) Dynamic mechanical analysis and its relationship to impact transitions. Polym Eng Sci 34:420–427
2. Djupfors R, Starck P, Lofgren B (1998) Copolymerization of propene with ethene by $Et(lnd)_2Hfcl_2$/methylaluminoxane catalyst. Eur Polym J 34:941–948
3. Lehtinen C, Starck P, Lofgren B (1997) Co-and terpolymerizations of ethene and a-olefins with metallocenes. J Polym Sci 35:307–318
4. Simanke AG, Galland GB, Freitas L, Jornada JAH, Quijada R, Mauler RS (1999) Influence of the comonomer content on the thermal and dynamic mechanical properties of metallocene ethylene/1-octene copolymers. Polymer 40:5489–5495
5. Nitta K, Suzuki K, Tanaka A (2000) Comparison of tensile properties in the pre-yield region of metallocene-catalyzed and Ziegler–Nattta-catalyzed linear polyethylenes. J Mater Sci 35:2719–2727
6. Kolesov IS, Androsch R, Radusch HJ (2004) Non-isothermal crystallization of polyethylenes as function of cooling rate and concentration of short chain branches. J Therm Anal Calorim 78:885–895
7. Starck P, Malmberg A, Lofgren B (2002) Thermal and rheological studies on the molecular composition and structure of metallocene- and Ziegler–Natta-catalyzed ethylene-a-olefin copolymers. J Appl Polym Sci 83:1140–1156
8. Kokko E, Malmberg A, Lehmus P, Lofgren B (2000) Influence of the catalyst and polymerization conditions on the long-chain branching of metallocene-catalyzed polyethenes. J Polym Sci 38:376–388
9. Wood-Adams PM, Dealy JM (2000) Effect of molecular structure on the linear viscoelastic behavior of polyethylene. Macromolecules 33:7489–7499
10. Wood-Adams PM, Costeux S (2001) Thermorheological behavior of polyethylene: effects of microstructure and long chain branching. Macromolecules 34:6281–6290

11. Garcia-Franco CA, Srinivas S, Lohse DJ, Brant P (2001) Similarities between gelation and long chain branching viscoelastic behavior. Macromolecules 34:3115–3117
12. Read DJ, Mcleish TCB (2001) Molecular rheology and statistics of long chain branched metallocene-catalyzed polyolefins. Macromolecules 34:1928–1945
13. Wood-Adams PM, Dealy JM (2000) Using rheological data to determine the branching level in metallocene polyethylenes. Macromolecules 33:7481–7488
14. Wang WJ, Ye Z, Fan H, Li BG, Zhu SP (2004) Dynamic mechanical and rheological properties of metallocene-catalyzed long-chain-branched ethylene/propylene copolymers. Polymer 45:5497–5504
15. Chen XH, Ma GQ, Li JQ, Jiang SC, Yuan XB, Sheng J (2009) Study on morphology evolution and fractal character of the miscible blend between isotactic polypropylene and copolymer of ethylene and propylene. Polymer 50:3347–3360
16. Gahleitner M, Hauer A, Bernreitner K, Ingolic E (2002) Polypropylene-based model compounds as tools for the development of high-impact ethylene–propylene copolymers. Intern Polym Proc 17:318–324
17. Da Silva ALN, Tavares MIB, Politano DP, Coutinho FMB, Rocha MCG (1997) Polymer blends based on polyolefin elastomer and polypropylene. J Appl Polym Sci 66:2005–2014
18. Bandyopadhyay GG, Bhagawan SS, Ninan KN, Thomas S (1999) Dynamic properties of NR/EVA polymer blends: model calculations and blend morphology. J Appl Polym Sci 72:165–174
19. Bandyopadhyay GG, Bhagawan SS, Ninan KN, Thomas S (1997) Viscoelastic behavior of NBR/EVA polymer blends: application of models. Rubber Chem Technol 70:650–662
20. Bandyopadhyay GG, Bhagawan SS, Ninan KN, Thomas S (2004) Viscoelastic behavior of polypropylene/nitrile rubber thermoplastic elastomer blends: application of Kerner's models for reactively compatibilized and dynamically vulcanized systems. J Polym Sci B 42:1417–1432
21. Kerner EH (1956) The elastic and thermo-elastic properties of composite media. Proc Phys Soc B 69:808–813
22. Mazich KA, PlummerJr HK, Samus MA, KillgoarJr PC (1989) Mean field calculations of the dynamic mechanical properties of two-phase elastomer blends: included particles in a matrix phase. J Appl Polym Sci 37:1877–1888
23. Mazich KA, Killgoar PC Jr, Ingram JA (1989) Mean-field calculations of the dynamic mechanical properties of heterogeneous elastomer blends. Rubber Chem Technol 62:305–314